AIP | Conference Proceedings

Numerical study of nonlinear, transcranial focused ultrasound wave propagation for blood-brain barrier (BBB) opening

Noé Jiménez, Bernardino Roig, Javier Redondo, Rubén Picó, Fabrice Marquet et al.

Citation: AIP Conf. Proc. **1481**, 155 (2012); doi: 10.1063/1.4757327
View online: http://dx.doi.org/10.1063/1.4757327
View Table of Contents: http://proceedings.aip.org/dbt/dbt.jsp?KEY=APCPCS&Volume=1481&Issue=1
Published by the American Institute of Physics.

Related Articles

Remarkable transmission characteristics of optical waves through modulated double-layered metallic slit arrays
AIP Advances 2, 042112 (2012)

Time-domain determination of transmission in quantum nanostructures
J. Appl. Phys. 112, 064325 (2012)

Wireless power transfer to a cardiac implant
Appl. Phys. Lett. 101, 073701 (2012)

A finite-difference time-domain simulation of high power microwave generated plasma at atmospheric pressures
Phys. Plasmas 19, 073503 (2012)

Near-field focused photoemission from polystyrene microspheres studied with photoemission electron microscopy
J. Chem. Phys. 137, 014202 (2012)

Additional information on AIP Conf. Proc.

Journal Homepage: http://proceedings.aip.org/
Journal Information: http://proceedings.aip.org/about/about_the_proceedings
Top downloads: http://proceedings.aip.org/dbt/most_downloaded.jsp?KEY=APCPCS
Information for Authors: http://proceedings.aip.org/authors/information_for_authors

ADVERTISEMENT



Downloaded 25 Oct 2012 to 158.42.71.212. Redistribution subject to AIP license or copyright; see http://proceedings.aip.org/about/rights_permissions

Numerical Study of Nonlinear, Transcranial Focused Ultrasound Wave Propagation for Blood-Brain Barrier (BBB) Opening

Noé Jiménez[a], Bernardino Roig[a], Javier Redondo[a], Rubén Picó[a], Fabrice Marquet[b], Elisa E. Konofagou[b,c] and Francisco Camarena[a]

[a]*Instituto para la Gestión Integrada de Zonas Costeras (IGIC), Universidad Politécnica de Valencia, Escuela Politécnica Superior de Gandía. Grao de Gandía, Valencia Spain*
[b]*Department of Biomedical Engineering, Columbia University, New York, NY USA*
[c]*Department of Radiology, Columbia University, New York, NY USA*

Abstract. Focused ultrasound (FUS) techniques for Blood-Brain Barrier opening are emerging for localized and safe brain drug delivery. In this work, a transcranial FUS field is computed by a numerical approach entailing nonlinear wave propagation in the time domain in order to determine the position of the true focus and the existence of reflections and resonances. A transducer with a curvature radius of 90 mm, and an aperture of 80 mm was simulated at a central frequency of 500 kHz. The computational method was a Finite-Difference Time-Domain (FDTD) implemented on nonlinear fluid model over a 2D Axis-symmetric domain. The boundary conditions were derived from the apparent density measurements based on a 3D CT scan acquisition performed on a *Macaca mulatta* primate. The study shows that nonlinear propagation shifts the peak pressure 3 mm away from the transducer when the pressure in the transducer increases from 2 kPa to 70 kPa. The focal shift is mainly due to the presence of the skull and dependent on the incidence angle of the ultrasonic beam. This study proposes a FDTD nonlinear numerical approach to study the propagation of ultrasonic waves through the skull, showing that nonlinear propagation can affect the position of the focal peak.

Keywords: transcranial focused ultrasound, ultrasound-induced blood-brain barrier opening, nonlinear acoustics, FDTD, finite difference time-domain
PACS: 43.80.Sh, 43.35.Wa, 87.50.yt, 02.70.Bf

INTRODUCTION

Over 95% of useful therapeutically molecules cannot penetrate to the brain parenchyma in central nervous system (CNS) due to the blood-brain barrier (BBB) [1]. This barrier is composed mainly by endothelial cells forming a tight structure, ensuring protection to injurious substances to the CNS. The cells of the endothelium are tightly bounded and these links are known as tight junctions (TJs). In recent years it has been developed a promising ultrasound assisted technique for noninvasive, targeted and safe BBB disruption (BBBD) for drug delivery [2, 3]. This technique employs a transcranial focused ultrasound beam focalized on targeted BBB areas to disrupt. An ultrasound contrast agent is needed to minimize the ultrasound pressure amplitude of the focused beam and ensure the BBB aperture without damaging the

11th International Symposium on Therapeutic Ultrasound
AIP Conf. Proc. 1481, 155-161 (2012); doi: 10.1063/1.4757327
© 2012 American Institute of Physics 978-0-7354-1093-0/$30.00

Downloaded 25 Oct 2012 to 158.42.71.212. Redistribution subject to AIP license or copyright; see http://proceedings.aip.org/about/rights_permissions

brain tissue. The transient BBB disruption is related to a mechanical effect due to the interaction of oscillating micro-bubbles and the endothelial TJs [1].

However, there are many limitations of the technique. The amplitude of the acoustic wave has to be low enough to ensure that the thermal effects due to the energy absorption do not damage the tissue. Likewise, because the ultrasound contrast agent contains micro-bubbles, the acoustic amplitude has to be under the inertial cavitation threshold of these bubbles [1]. Nevertheless, there are some works that induce cavitation to successfully opening the BBB [5]. On the other hand, the skull shows very high acoustic absorption at interest frequencies, and the acoustic impedance of the skull bone is highly different than the inner brain and outer media [6, 7], so the acoustic wave amplitude must be high enough to counteract these effects. Patient-specific shape of the skull produces aberrations in the acoustic field generated by focused acoustic beams that cause unexpected targeted focal areas [6, 8]. Finally, a shift in the position of the focal peak is related to the linear behavior of the acoustic wave [9] and this shift can be affected by the nonlinear behavior of the acoustic waves through nonlinear media like brain tissue [10]. Although the wave amplitude for ultrasound assisted BBBD must be relatively small, nonlinear effects can affect the position of the focal peak in nonlinear media. Thus, the main aim of this work is to quantify the nonlinear shift effect in transcranial propagation and to compare this effect with the linear shift due to the phase aberrations of the skull. In order to do this, a computational method based on Finite-Differences in Time-Domain (FDTD) is developed and applied to the nonlinear acoustic equations for a viscous fluid.

PHYSICAL MODEL

Intracranial propagation of ultrasound waves implies that waves are backscattered inside the skull bone layer in a wide variety of angles. Hence, a volumetric model that provides arbitrary boundary and initial conditions, arbitrary wave propagation direction, and no paraxial approximations is needed. Although shear elasticity is present in bones and soft tissue, when the incidence angle of the main beam is within about 20º of normal, the mode conversion from longitudinal to shear waves is negligible, at least in the beam axis direction [14] and a fluid model considering only longitudinal waves can realistically describe the problem. Therefore, the proposed model only supports longitudinal nonlinear waves. The main equations of the model to nonlinear acoustics are taken from conservative principles over a fluid control volume. Thus, neglecting body forces and thermal effects, the conservation of mass, momentum, and an adequate fluid state relation leads to the following expressions [15]:

$$\frac{\partial \rho}{\partial t} + \nabla \cdot (\rho \mathbf{v}) = 0 \tag{1}$$

$$\rho\left(\frac{\partial \mathbf{v}}{\partial t} + (\mathbf{v}\nabla)\mathbf{v}\right) + \nabla p - \eta \nabla^2 \mathbf{v} - \left(\zeta + \frac{1}{3}\eta\right)\nabla(\nabla \cdot \mathbf{v}) = 0 \tag{2}$$

$$p' = c_0^2 \rho' + \frac{c_0^2}{\rho_0}\frac{B}{2A}\rho'^2 \tag{3}$$

Downloaded 25 Oct 2012 to 158.42.71.212. Redistribution subject to AIP license or copyright; see http://proceedings.aip.org/about/rights_permissions

Where ρ is the total density, **v** is the vector particle velocity, p is the total pressure, η and ζ are the shear and bulk viscosities, B/A is the nonlinearity parameter and c_0 is the small signal sound speed. Due to the fact that a rectilinear 3D coordinate system would increment the total computational cost, in this work a cylindrical axisymmetric coordinate system has been applied. As counterpart, the boundary conditions of the primate skull are approximate as a body of revolution of a CT scan slice so the numerical results presented on this study are not comparable to experimentally measured acoustic fields inside a real skull. However, this approach can be used to study the magnitude of the nonlinear effects.

NUMERICAL MODEL

Numerical simulation is performed by a modified Finite-Differences Time-Domain (FDTD) method (more details about the FDTD method can be seen in [16]). The nonlinear model equations are based on conservative laws, and hence, to ensure the consistence of the numerical method, a conservative discretization all over the discrete cells must be done [17]. This conservative discretization implies that for each cell the conservation laws must be fulfilled. As a consequence, the initial explicit method turns into an implicit one. An iterative method is applied for the solver and time-steeping is developed by a "Leap Frog" algorithm. The iterative method converges quickly due to the linear solution of the system is known by a standard FDTD scheme, i.e. with only 2 iterations the relative error to the exact solution is below -100 dB. The consistent presented non-linear numerical method has a stability condition similar to the standard FDTD. Because the amplitude of the acoustic wave for BBBD is near the linear regime, the natural viscosity of the fluid avoids the higher harmonics and a grid of 35 elements per wavelength is a sufficient condition to ensure nonlinear stability.

BOUNDARY CONDITIONS

A focused transducer with a curvature radius of 90 mm and an aperture of 80 mm was simulated at a central frequency of 500 kHz and was placed focusing at the interior of the skull at a depth of 30 mm from the skull surface and with a normal incidence angle. The skull boundary conditions were deduced from the CT apparent density images obtained from a GE LigthSpeed VCT 64 scanner (GE Medical Systems, Milwaukee, WI) with a native 488-μm resolution and slice of 625 μm. Thus, CT scans over a rhesus monkey (*Macaca mulatta*). Sound speed and density maps were obtained from the normalized apparent CT density [6], and the mean values are listed in table 1:

TABLE 1. Parameters of the numerical simulation

Skull parameter		**Value**	**Water parameter**		
Density (kg / m^3)	$\rho_{\max}$	2190	Density (kg / m^3)	ρ_{water}	1000
Sound speed (m / s)	c_{max}	3100	Sound speed (m / s)	c_{water}	1540
Attenuation (Np / m)	α	50	Shear viscosity (Pa·s)	η	$0.894 \cdot 10^{-3}$
			Bulk viscosity (Pa·s)	ζ	$2.43 \cdot 10^{-3}$
			Nonlinear parameter	B/A	4.96

Downloaded 25 Oct 2012 to 158.42.71.212. Redistribution subject to AIP license or copyright; see http://proceedings.aip.org/about/rights_permissions

Because of the axis-symmetric coordinate system employed, only a slice of the CT map is required. Figure (1) shows the selected plane and its location on the 3D skull, the focused transducer axis and geometric focus.

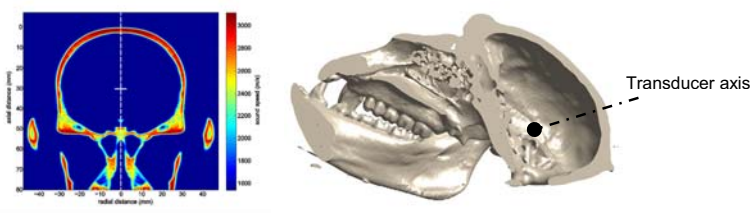


FIGURE 1. 3D representation of the CT scan map, transversal cut of an isosurface at density value of 1238 kg/m^3. The dashed line shows the transducer axis and the focal point. The slice for the 2D axisymmetric is determined by cut-plane of the transducer axis.

VALIDATION OF THE FDTD MODEL

The linear validation of the numerical scheme is performed by comparison with analytical solution of the on-axis pressure envelope of a focused ultrasound transducer [9]. At N>20 elements/λ the relative error is below 0.24% for the effective focal position and below 0.29% for the peak pressure amplitude in the focus. The nonlinear validation of the numerical code was done by comparison with several analytical solutions for a plane wave, and for a resolution of N=32, the relative error was below 1.67% in pre-shock (Bessel-Fubini) and below 2.80% for post-shock (Blackstock-Fay) region [15, 18].

RESULTS

Linear effects: A simulation at very low input amplitude (0.1 Pa) was done in order to quantify the effects of the wave propagation in transcranial application in linear regime. Another, simulation was performed in water without the primate skull to determine the influence of the skull in the position of the focal area (Table 2).

TABLE 2. Beam properties for the linear simulations in water with and without skull.

Media	**Focal** (mm)	**Focal shift** (mm)	**Beamwidth axial** (mm)	**Beamwidth radial** (mm)	**Effective Gain** (P_0 / P_{focal})
Water	87.4	-2.6	34.7	4.8	18.34
Water with skull	84.9	-5.1	32.8	4.8	1.67

Nonlinear effects: Several simulations were performed in water in order to determine the position of the transducer focus in absence of the primate skull and the input pressure dependence. Peak pressure location for compression and for rarefaction was determined. Figure 2.a) shows these locations versus the input pressure, showing that the input pressure can affect the location of the position of these maxima. This effect is called as nonlinear shift, and in this experiment can displace the compression effective focus +1.35 mm away from the linear focus, and the minimum rarefaction shift -3.37 mm from the linear focus. At lower pressures the value of the nonlinear

Downloaded 25 Oct 2012 to 158.42.71.212. Redistribution subject to AIP license or copyright; see http://proceedings.aip.org/about/rights_permissions

shift matches with the linear shift predicted by the analytic linear solution by a difference of 0.0050 mm.

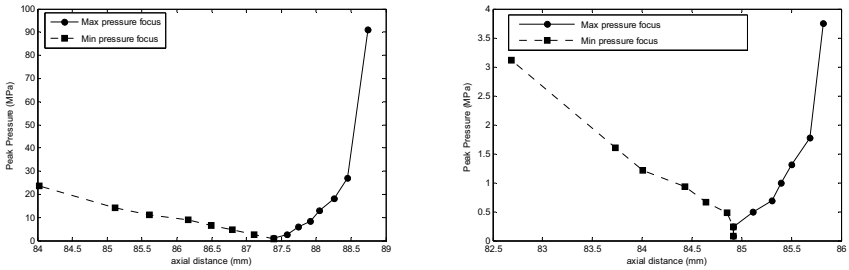


FIGURE 2. Peak location vs. input pressure. a) simulation in water, b) simulation with skull. Continuous circles: peak compression location; dotted squares: minimum rarefaction location. The geometric focus is 90 mm.

New simulations were performed with the skull inhomogeneities at the same input pressure amplitudes. Figure 2.b) plots the nonlinear behavior of the focal position into the skull. The nonlinear propagation displaces the compression peak until 0.90 mm respect to the linear position and 2.24 mm from the rarefaction peaks.

Due to the asymmetry of the wave profile, the effective gain of the transducer (P_0/P_{focus}) is different for peak pressure and for minimum pressure peak. The gain for the water simulations with and without skull is shown in Figure 3. Due to the skull insertion losses, the effective gain of the transducer for the transcranial application was very low compared to the gain in water, but beyond this, the nonlinear behavior of the gain for compression and rarefactions is analogous. On water, the increment on gain for compression peak is in the range from 1.02 to 2.48 times the linear gain of the transducer, and 0.99 to 0.65 times the linear gain for rarefaction minimum pressure. On skull, the gain variations range from 1.01 to 1.24 times the linear gain for compression pressure and from 1.00 to 0.93 on rarefaction.

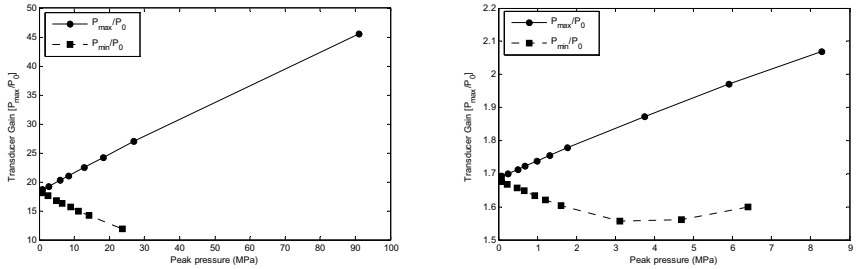


FIGURE 3. Nonlinear effective gain for a) water simulation, and b) transcranial simulation. Continuous circles: peak compression gain; dotted squares: minimum rarefaction gain. The linear gain is 18.34 for water and 1.67 for transcranial simulations.

Finally, half-power beamwidth is analyzed for the different input pressures, in water and in skull media. Figure 4.a) shows the beamwidth for the compression and for rarefaction in water. As the wave amplitude increases, the beamwidth for compression becomes narrower, ranging from 4.4 to 2.8 mm (-37.5% variation) for lateral width and from 28.9 to 34.4 mm (-31.3% variation) for axial width. In contrast, the targeted area for rarefaction increases from 34.8 to 40.8 mm (+17.1%) for axial and from 4.8 to 6.0 mm (+24%) for lateral. This behavior has been observed for the

Downloaded 25 Oct 2012 to 158.42.71.212. Redistribution subject to AIP license or copyright; see http://proceedings.aip.org/about/rights_permissions

skull simulations as shown in Figure 4.b), and the beamwidth values for compression ranges from 4.8 to 4.2 mm (-12.0%) for lateral and from 32.4 to 29.0 mm (-11.0%) for axial width. For rarefaction, the beamwidth varies from 4.8 to 5 (+4.0%) mm for lateral and from 30.1 to 32.2 (+10.8%) mm for axial width.

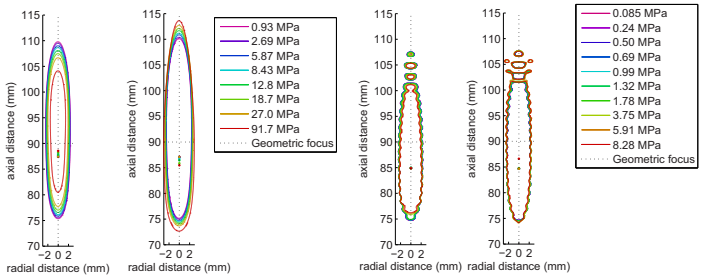


FIGURE 4. a) Beamwidth for water simulation: a.1) compression, a.2) rarefaction. b) Beamwidth for transcranial simulations: b.1) compression, b.2) rarefaction.

CONCLUSIONS

A numerical method for ultrasound transcranial simulation in nonlinear regime has been developed and validated with analytical solutions. The method has been employed for computing focused ultrasound acoustics fields in water and in water with a primate skull for a BBBD application. The results shown that, at frequency of 500 kHz and at interest pressures (0.1 MPa to 1 MPa), the beam properties can be affected by the acoustic nonlinearities. The targeted area, i.e. the focal position and the beamwidth, and the gain for the BBBD varies due to the amplitude of the wave. Moreover, this behavior is different for the compression and the rarefaction peaks. These effects can be important in many practical situations, i.e. when it comes time to predict if the beam amplitude overcomes the cavitation threshold, or for accurate quantify the sonification area for focused ultrasound assisted BBBD treatment.

ACKNOWLEDGMENTS

This work was supported by the Spanish Government, under the Project FIS2008-06024-C03-03 and Programa de Apoyo a la Investigación y Desarrollo of the Universidad Politécnica de Valencia PAID-06-10-002-295, Spain.

REFERENCES

1. Hynynen, K. *Adv. Drug. Deliv. Rev.* **60** 1209-1217 (2008).
2. L. Bakay, T.F. Hueter, H.T. Ballantine and D. Sosa, *Arch. Neurol*. **76**, 457-467. (1956)
3. G. Mychaskiw, A.E. Badr, R. Tibbs, B.R. Clower and J.H. Zhang.*Anesth. Analg.* **91**,798-803 (2000)
4. N. McDannold, N. Vykhodtseva, F.A. Jolesz and K. Hynynen, *Magn Reson.Med.***51**,913-923 (2004)
5. N. McDannold, N. Vykhodtseva, and K. Hynynen, *Phys. Med. Biol.,* **51**-4, 793-807 (2006)
6. E. E. Konofagou and T. Deffieux, *IEEE T Ultrason. Ferr.* **57**(12) 2637 - 2653 (2010)
7. F.J. Fry and J. E. Barger, *J. Acoust. Soc. Am.* **63**(5), 1576-1590 (1978)
8. J. F. Aubry, M. Tanter, M. Pernot, J. L. Thomas, and M. Fink, *J.Acoust.Soc.Am.***113**(1),84-93 (2003)
9. H. T. O'Neil. Theory of Focusing Radiators. *J. Acoust. Soc. Am.* **21**(5), 516 (1949)

Downloaded 25 Oct 2012 to 158.42.71.212. Redistribution subject to AIP license or copyright; see http://proceedings.aip.org/about/rights_permissions

10. Y. N. Makov, V. Espinosa, V. J. Sánchez-Morcillo, J. Ramis, J. Cruañes, and F. Camarena. *J. Acoust. Soc. Am.* **119**(6), 3618-3624 (2006)
11. F. Marquet, M. Pernot, J. F. Aubry, G. Montaldo, L. Marsac, M. Tanter, and M. Fink, *Phys. Med. Biol.*, **54**(9) 2597-2613 (2009)
12. J. J. Kaufman, G. Luo, and R. S. Siffert. *IEEE T Ultrason. Ferr.* **55**(6) 1205 (2008)
13. E. Bossy, M. Talmant, and P. Laugier, *J. Acoust. Soc. Am*. **115**(5) (2004)
14. P. J. White, G. T. Clement, and K. Hynynen, *Ultrasound Med. Biol.* **32**(7) 1085-1096 (2006)
15. K. A. Naugolnykh and L. A. Ostrovskii. *Nonlinear Wave Processes in Acoustics*. Cambridge University Press, New York, NY. (1998)
16. A. Taflove and S. Hagness. *Computational Electrodynamics. The Finite Difference Time Domain method,* 3ª ed. North Artech House Inc. (2005)
17. R. J. LeVeque, *Numerical Methods for Conservation Laws*, Birkhauser-Verlag, Basel, Lectures in Mathematics, ETH-Zurich, 1990
18. M. F. Hamilton, D. T. Blackstock. *Nonlinear Acoustics: Theory and Applications*. Academic Press. 1st edition (1997)

Downloaded 25 Oct 2012 to 158.42.71.212. Redistribution subject to AIP license or copyright; see http://proceedings.aip.org/about/rights_permissions